LETTER

ELM elimination with Li powder injection in EAST discharges using the tungsten upper divertor

IOP Publishing | International Atomic Energy Agency Nuclear Fusion

Nucl. Fusion **58** (2018) 024003 (7pp) https://doi.org/10.1088/1741-4326/aa9e3f

Letter

ELM elimination with Li powder injection in EAST discharges using the tungsten upper divertor

R. Maingi[1,a], J.S. Hu[2,a], Z. Sun[2], K. Tritz[3], G.Z. Zuo[2], W. Xu[2], M. Huang[2], X.C. Meng[4], J.M. Canik[5], A. Diallo[1], R. Lunsford[1], D.K. Mansfield[1], T.H. Osborne[6], X.Z. Gong[2], Y.F. Wang[2], Y.Y. Li[2] and EAST team[b]

[1] Princeton Plasma Physics Laboratory, 100 Stellarator Road, Princeton, NJ 08540, United States of America
[2] Institute of Plasma Physics, Chinese Academy of Sciences, Hefei, Anhui 230031, People's Republic of China
[3] Johns Hopkins University, Baltimore, MD 21211, United States of America
[4] Department of Applied Physics, Hunan University, Changsha 410082, People's Republic of China
[5] Oak Ridge National Laboratory, Oak Ridge, TN 37830, United States of America
[6] General Atomics, San Diego, CA 92121, United States of America

E-mail: rmaingi@pppl.gov and hujs@ipp.ac.cn

Received 26 August 2017, revised 26 November 2017
Accepted for publication 29 November 2017
Published 5 January 2018

Abstract

We report the first successful use of lithium (Li) to eliminate edge-localized modes (ELMs) with tungsten divertor plasma-facing components in the EAST device. Li powder injected into the scrape-off layer of the tungsten upper divertor successfully eliminated ELMs for 3–5 s in EAST. The ELM elimination became progressively more effective in consecutive discharges at constant lithium delivery rates, and the divertor D_α baseline emission was reduced, both signatures of improved wall conditioning. A modest decrease in stored energy and normalized energy confinement was also observed, but the confinement relative to H98 remained well above 1, extending the previous ELM elimination results via Li injection into the lower carbon divertor in EAST (Hu *et al* 2015 *Phys. Rev. Lett.* **114** 055001). These results can be compared with recent observations with lithium pellets in ASDEX-Upgrade that failed to mitigate ELMs (Lang *et al* 2017 *Nucl. Fusion* **57** 016030), highlighting one comparative advantage of continuous powder injection for real-time ELM elimination.

Keywords: edge localized modes, plasma wall interactions, lithium seeding, edge stability

(Some figures may appear in colour only in the online journal)

1. Introduction

Ever since the discovery of the high-confinement mode (H-mode) regime in fusion devices [1], periodic relaxation events in the edge plasma have been observed; these events result in edge plasma ejections and are termed edge-localized modes (ELMs) [2]. While ELMs beneficially flush out impurities from the edge, they also result in high transient and periodic plasma loads to plasma-facing components (PFCs). These particle and heat loads can lead to enhanced erosion, thermal cycling fatigue, and reduced lifetime of PFCs [3, 4]. One categorization of the severity of ELMs is the fractional plasma stored energy loss, $\Delta W/W_{\rm tot}$ where ΔW is the energy loss and

[a] The first two authors should be considered as equal co-authors.
[b] The full EAST listing is available in B.N. Wan *et al* [32].

W_{tot} is the plasma stored energy prior to the ELM. Note that the best H-mode plasma energy confinement is often correlated with large ('Type I') ELMs; these ELMs can have $\Delta W/W_{tot}$ up to 0.1–0.15 per ELM [5]. Projected toward ITER using collisionality scalings, these unmitigated ELMs would result in unacceptable damage to PFCs. Measured energy fluences to divertor targets can also be used to extrapolate to ITER; these scalings project [6] to smaller unmitigated ELMs in ITER than simple collisionality scalings. Thus research on ELM size reduction or on ELM elimination techniques continues [7–9].

ELM heat flux can be mitigated by pellets (fuel [10, 11] or impurity [12–16]) or magnetic perturbations [17, 18], by pacing ELMs at rates faster than the natural ELM frequency and relying on an inverse relationship between peak heat flux and ELM frequency. ELMs can also be passively suppressed by operation in regimes devoid of natural ELMs, e.g. QH-mode [19] and I-mode [20]. Alternately ELMs can be actively suppressed via e.g. magnetic perturbations [21, 22], or with Li conditioning [23, 24] and/or active Li injection [25], the subject of this Letter.

ELMs were eliminated in previous EAST experiments with real-time Li aerosol injection onto graphite PFCs in the lower divertor [26], albeit with modest H-mode confinement factor of 0.75 relative to IPB98(y,2) scaling [27]. In those experiments the relative importance of real time aerosol injection and cumulative wall conditioning/reduced recycling was not determined. To the extent wall conditioning is an important element, one would expect a difference between porous PFCs like graphite, and refractory metals like W. In principle the efficacy of Li *conditioning* on graphite surfaces is limited, due to intercalation of Li into the graphite pores. In this regard Li application to refractory metals like W should be more effective and long-lived than application on porous materials. Hence there is substantial interest in extending the early EAST results, both to discharges that use high-Z PFCs, to see if a conditioning effect becomes more obvious, and also to higher confinement discharges. However, recent Li seeding experiments with large pellets in ASDEX-Upgrade with all W PFCs showed *no intrinsic benefit* of high Li concentrations in the plasma. In particular the H-mode pedestal characteristics and ELM behavior were unaffected in ASDEX-Upgrade, even with Li core concentrations up to 10–15% [28]. A short-lived conditioning effect was observed, but large scale conditioning improvement was obviated by the low Li doses employed.

In this Letter, we present the first successful elimination of ELMs with real time Li powder injection using the tungsten upper divertor in EAST. Moreover these discharges exhibited good energy confinement, with confinement relative to the IPB98(y,2) scaling [27] >1, and there is clear evidence of a cumulative wall conditioning effect. An overview of experiments is given in section 2, and a summary and outlook is presented in section 3.

2. Overview of experiments

The goals of the experimental advanced superconducting tokamak (EAST) include execution of long pulse, high performance H-mode discharges [29, 30] heated mainly by radio frequency (RF) heating and deploying high-Z PFCs prototypical of reactors [31], e.g. the use of ITER W mono-block technology. The machine has major radius $R = 1.85$ m, minor radius $r \leqslant 0.5$ m, with an eventual goal of 1000 s long pulse length. The move toward high-Z PFCs is occurring in a staged implementation; the device used all graphite PFCs until 2012; then the central column tiles were changed to Mo, and recently the upper divertor tiles were replaced with W mono-block [32]. To achieve long pulse recycling and impurity control, Li wall conditioning is deployed, via a combination of overnight evaporation and periodic use of real time Li powder or granule injection [33, 34]. The combination of these capabilities resulted in H-mode discharges with duration in excess of 60 s [35].

In addition to recycling control and confinement enhancement, real-time Li powder injection [25] into discharges on graphite PFCs succeeded in eliminating ELMs [26]. Interaction between the injected powder and plasma effectively creates a Li aerosol. The first EAST results exhibited many similarities to ELM elimination via pre-discharge Li evaporation on NSTX [36], where a cumulative wall conditioning effect was clearly observed. The first EAST results also showed similarities to the extension of the inter-ELM period and improved confinement with Li injection on DIII-D [37]; in the DIII-D case, however, there was no cumulative conditioning effect observed, but rather stimulation of pedestal localized magnetohydrodynamic (MHD) activity. We note that the stimulated MHD activity was distinct from the edge harmonic oscillation observed in quiescent H-mode [19] in DIII-D. Thus the staged move toward high-Z PFCs in EAST posed a new challenge: could ELMs be eliminated when the principle plasma-material interaction was occurring on a high-Z surface, in light of the recent seeding experiment with large Li pellets in ASDEX-Upgrade [28]?

Two Li powder droppers were implemented in the upper ports of the EAST device to determine if the previous ELM elimination on the graphite PFCs could be extended to discharges using the upper divertor W mono-block as the primary PFCs. EAST typically deploys a daily 10–30 g coating of Li via evaporation, but this coating has a finite duration before losing effectiveness [30]. Note that this coating dose substantially exceeds the dose injected via the dropper (typically a few hundred mg during a discharge), indicating that the real time dropper injection is more efficient in altering the plasma behavior; similar behavior was observed in NSTX [38]. There are unfortunately no direct measurements of Li density in the core to confirm this. The poloidal location of the two injectors, one on the high-field side (HFS) just above the X-point and one on the low-field side (LFS), along with an upper single-null equilibrium (from the second discharge with Li injection, #70592, but the same shape was used in all of the discharges in this paper) are shown in figure 1. In these discharges, only the LFS injector was used. Also shown in figure 1 are unfiltered tangential charge-coupled device (CCD) color camera images of plasma emission before and after real-time Li injection was used in an H-mode discharge. The red colors indicate both D_α (656 nm) and Li-I (671 nm) light, while the yellow/orange (Li-I 610 nm) and green (Li-II

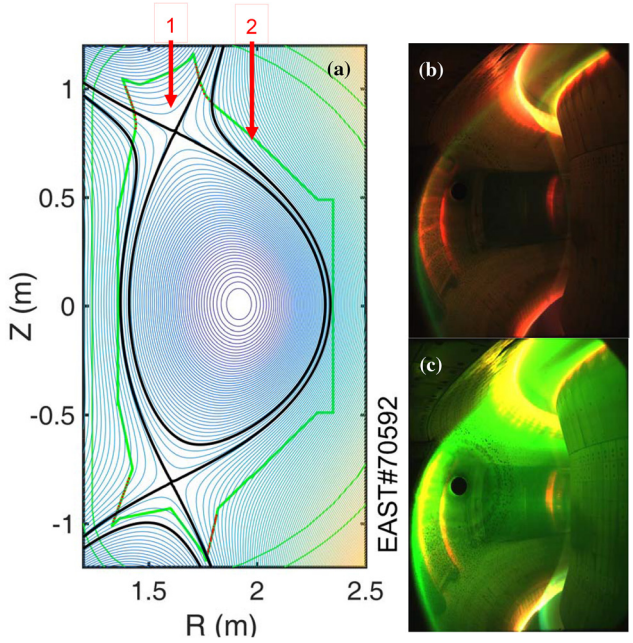

Figure 1. (*a*) reconstructed equilibrium from an upper-single null divertor discharge #70592, with two dropper locations schematically indicated; visible color camera images obtained (*b*) before and (*c*) during Li powder injection. The color CCD camera has three sensors, to supply true RGB color (model AT-200Cl, www.jai.com/en/products/at-200cl).

548 nm) are from Li line emission. The residual upper divertor yellow/orange and green light in the time slice before Li injection is from residual Li from the daily morning evaporation.

Figure 2 compares two discharges with matched heating power, with and without real Li injection, demonstrating that ELMs were gradually eliminated with the use of real-time Li injection. The discharge control parameters were: plasma current $I_p = 0.4$ MA, toroidal field $B_t = -2.5$ T, and ion grad-B drift away from the upper X-point, i.e. in the 'unfavorable' drift direction for H-mode access, and a physical separation of the two X-points of 2.0 cm at the outer midplane ('drsep'). Auxiliary heating included 2.0 MW lower hybrid heating @ 4.6 GHz, 0.4 MW lower hybrid heating @ 2.45 GHz, 0.3 MW electron cyclotron resonant heating (ECRH), at a program line-integral density $n_e \sim 2.8 \times 10^{19}$ m^{-3}. The LFS Li dropper was activated from 3.5 to 8 s in #70592, injecting about 80 mg s^{-1} (6.88×10^{21} Li atoms s^{-1}) of nominal 45 μm diameter spherical powder into the scrape-off layer (SOL); in comparison, the assumed electron inventory in a typical EAST plasma is 3×10^{20}. Note that while nearly 100% of the Li powder is ionized in the SOL, only a small fraction typically penetrates into the main chamber, leading to Li ion concentrations of up to 15% in DIII-D [37] and ASDEX-Upgrade [28]; as mentioned earlier, a direct measurement is unavailable in EAST. The ELM frequency in the reference discharge #70597 was ~200 Hz, as indicated by the 'spikes' in the upper divertor D_α emission in panel (*e*), and the baseline D_α emission was higher than in #70592 because #70597 followed a high density ohmic conditioning pulse. Nonetheless #70597 is a representative ELMy H-mode suitable as a reference. Use of the Li dropper resulted in ELM elimination from 3.5–8 s (panel (*f*)). Note that the large D_α blips seen for $t \geqslant 4$ s in panel (*f*) originate from short neutral beam pulses for charge-exchange measurements; the commonly-used neutral beam pulse technique has been described previously [39]. Curiously, the electron density measured by the polarimeter–interferometer (POINT) system [40] is temporarily reduced in #70592 around the time of the pulses, but not in the reference #70597. The reason for the transient density decreases is left as a scientific curiosity, but does not significantly affect the ELM elimination result. The gradual elimination of ELMs can also be observed by the narrowing envelope of the ion saturation current from a Langmuir probe embedded in the upper divertor near the outer strike point (panels (*k*) and (*l*)), which are obtained at 50 kHz sampling rate.

Although the radiated power was markedly higher in the discharge with the Li dropper (panel (*h*)), but this was not correlated with the dropper activation, and was still <20% of the total heating power in both discharges. Instead the core W line emission (panel (*i*)) was higher early in the dropper discharge, likely due to moderately higher W sputtering before the dropper was activated. Note also that while the normalized energy confinement (panel (*j*)) was reduced by up to 5–10% using the Li dropper, the overall enhancement over IPB98(y, 2) scaling [27] remained at ~1.2. The normalized confinement here was about 50% higher than the H98 ~ 0.75 obtained during ELM elimination with Li aerosol injection into the lower carbon divertor in the previous ELM elimination experiments [26].

An expanded time base of the ion saturation current from upper divertor Langmuir probes and dB/dt from a Mirnov probe are compared for the reference and Li dropper discharges in figure 3. It can be seen that ELM activity is manifest as spikes in both the ion saturation current and Mirnov data in the reference discharge (panels (*a*)–(*c*)), and in the Li discharge before Li injection (panel (*d*)). These spikes are absent from the Li dropper discharge after ELM elimination (panels (*e*) and (*f*)). It should be noted that the probes plotted in panels 3(*e*) and (*f*) are adjoining probes, because the equilibrium shifted by a few cm during the discharge evolution. Hence the closest probe to the strike point is plotted in those two panels. The elevated baseline in panel 3(*f*) relative to panel 3(*e*) originates from the fact the probe data in panel 3(*f*) is closer to the equilibrium strike point during the sampled time than the probe data in panel 3(*e*).

A progressive wall conditioning effect of the droppers was observed in these experiments, as documented with the previous dropper experiments in EAST [26] and also with progressively increasing evaporative coatings in NSTX [41]. Figure 4 shows three sequential discharges using the same programmed Li dropper rates, compared with the reference discharge; note that the middle discharge in this sequence #70592 was highlighted in figures 2 and 3. ELMs were eliminated at $t = 4.8$ s in the first discharge (#70591, panel (*b*)), at $t = 3.5$ s in the second discharge (#70592, panel (*c*)), and even prior to Li dropper activation in the final discharge (#70593, panel (*d*)). The baseline D_α level was also progressively reduced, indicating both reduced density and recycling. Preliminary recycling and core fueling analysis with the SOLPS code indicated that the divertor recycling coefficient decreased by about 20%

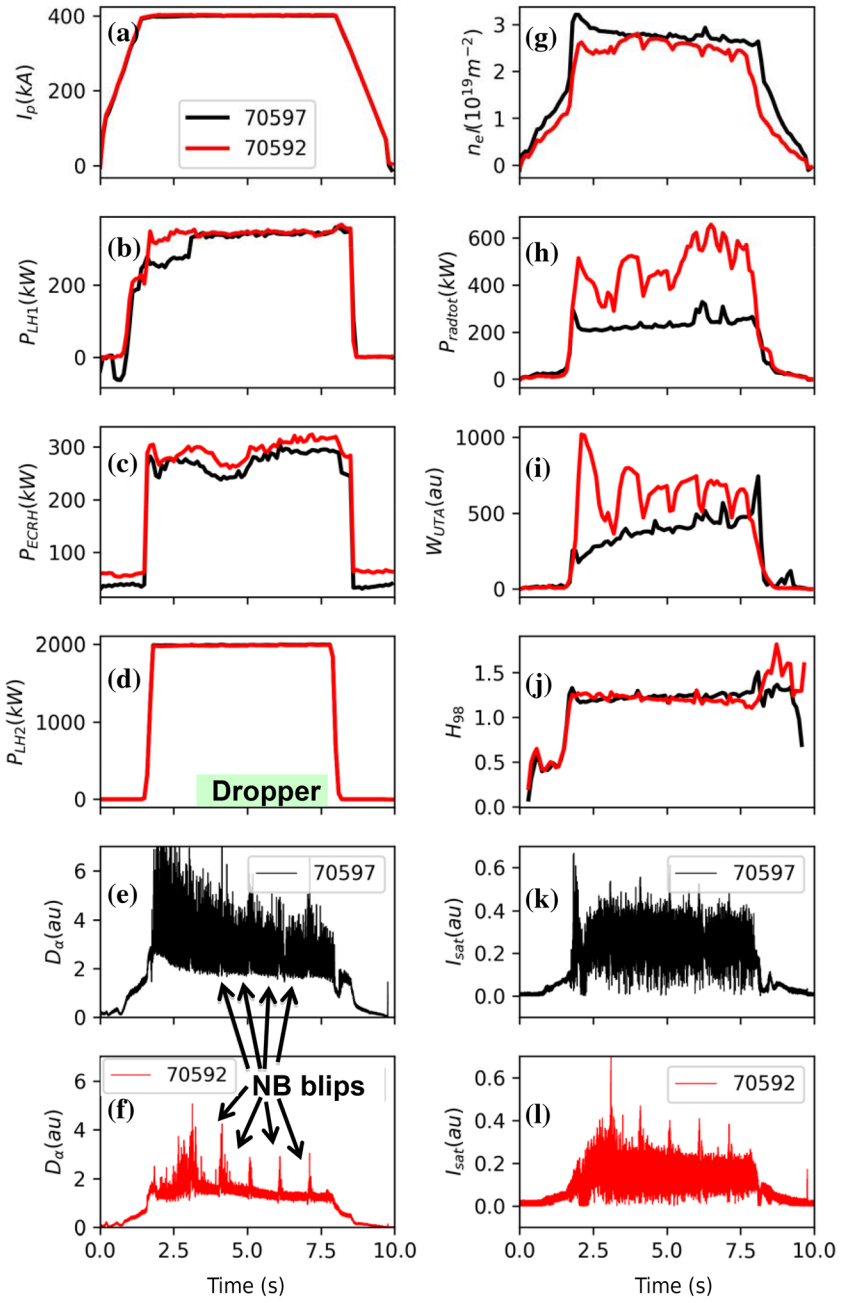

Figure 2. Time traces comparing reference (#70597—black) ELMy H-mode and one with Li powder injection (#70592—red): (*a*) plasma current I_p, (*b*) lower hybrid heating power @ 2.45 GHz P_{LH1}, (*c*) ECRH power P_{ECRH}, (*d*) lower hybrid heating power @ 4.6 GHz P_{LH1}, (*e*) and (*f*) upper divertor D_α emission, (*g*) line-average density n_{el}, (*h*) total radiated power $P_{radtot}t$, (*i*) core *W* line emission W_{UTA}, (*j*) confinement relative to IPB98(*y*,2) scaling H98, (*k*) and (*l*) ion saturation current from a tile-mounted Langmuir probe in the upper divertor near the outer strike point. The dropper was initiated at $t = 3.5$ s in #70592. Diagnostic neutral beam pulses were used at $t = 4$, 5, 6, 7 s in each discharge.

during the course of these discharges [42]. The rise of Li-II light reflects use of the dropper in panel (*e*).

While we observed progressive recycling reduction at fixed Li injection rate, this did not equate to continued confinement improvement in these discharges; in this sense these results differ from the progressive confinement improvement in NSTX [41]. The stored energy and electron density in the discharges with the dropper was reduced by up to 10% up to $t = 7.5$ s (panels (*f*) and (*g*)). In the third discharge #70593, an H–L transition occurred just after 7.5 s, suggesting that the Li injection was too high under the discharge conditions, as also observed at high injection rates in DIII-D [37]. Future experiment will seek to tailor the time dependence of the Li injection rate to provide ELM elimination with minimal impact on confinement. Nonetheless it should be kept in mind that the H98y2 ~ 1.1–1.2 represent very good H-mode confinement.

Figure 5 shows a plasma radial profile comparison for #70592 and #70597 for n_e, T_e, and T_i. The discharge with the Li dropper had modestly lower central n_e, and comparable core and edge T_e, with an H-mode pedestal-top temperature of ~400 eV. The discharge with Li injection exhibited ~20% higher T_i in the core. There was no obvious difference in the H-mode pedestal n_e value, and no data are available for the

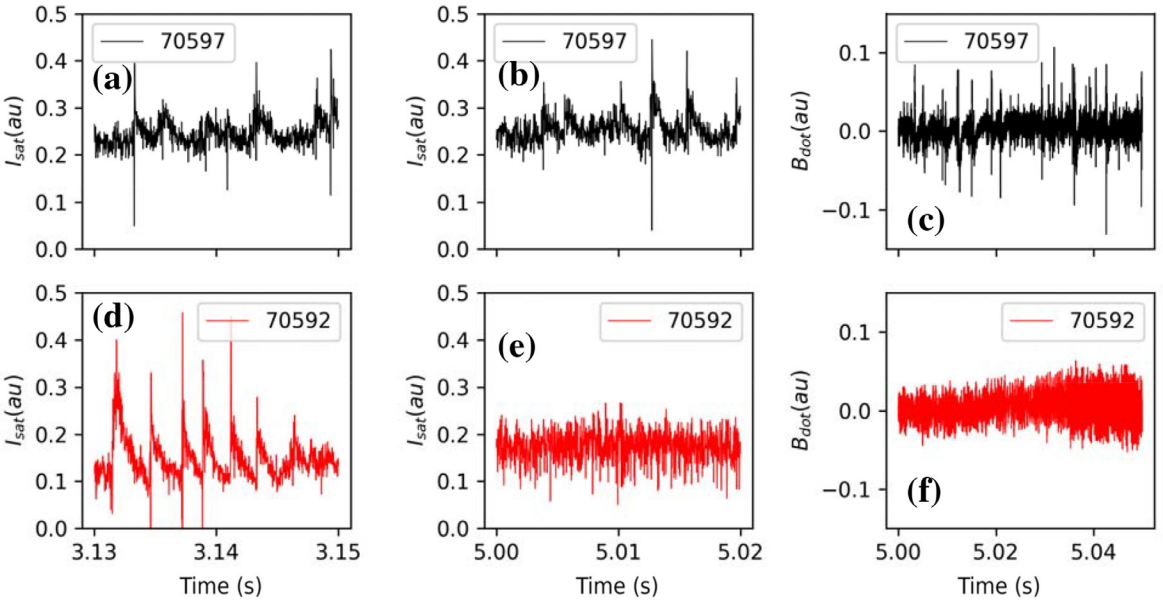

Figure 3. Comparison of ELM activity in reference and ELM eliminated discharges with the Li dropper: (*a*) tile-mounted upper divertor Langmuir probe ion saturation current I_{sat} (before Li injection), (*b*) I_{sat} (before Li injection), and (*c*) Mirnov probe signals. Panels (*a*)–(*c*) are for the reference ELMy discharge, while panels (*d*)–(*f*) are for the corresponding discharge with the LI dropper with (*d*) before and (*e*) and (*f*) after the start of Li injection.

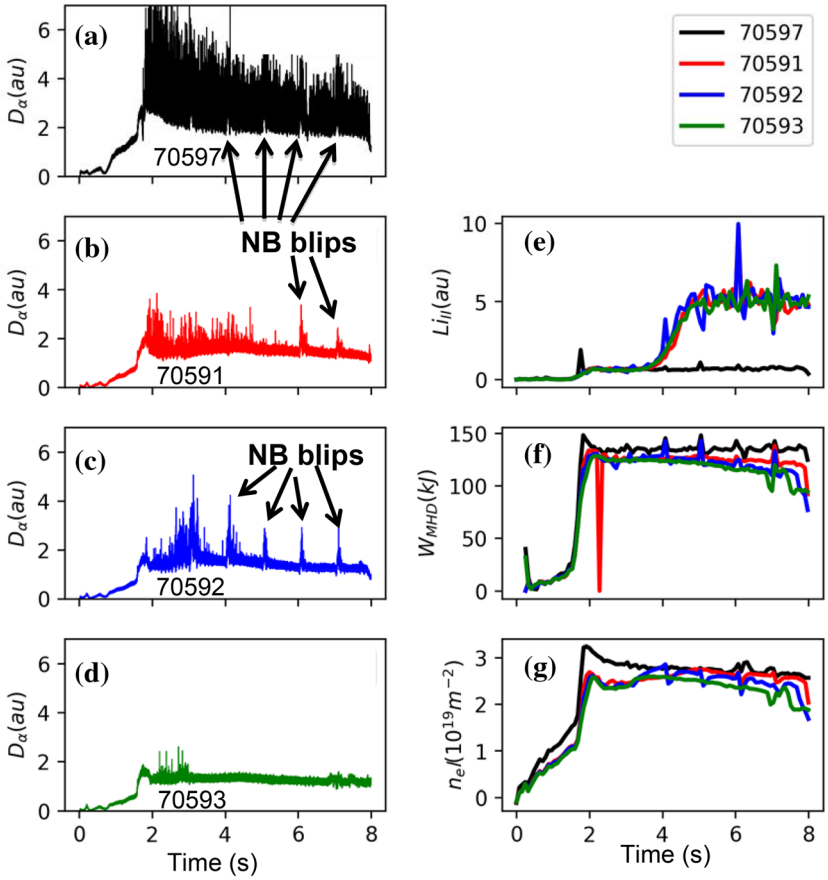

Figure 4. Upper divertor D_α emission from (*a*) reference #70597, (*b*) first discharge with dropper #70591, (*c*) second discharge with dropper #70592, (*d*) third discharge with dropper #70593. Also shown in panel (*e*) is the Li-II line emission (*f*) the plasma stored energy W_{MHD}, and (*g*) the line density from the POINT diagnostic. Note that the discharge #70593 had a pre-programmed extended pulse length as compared with the other discharges.

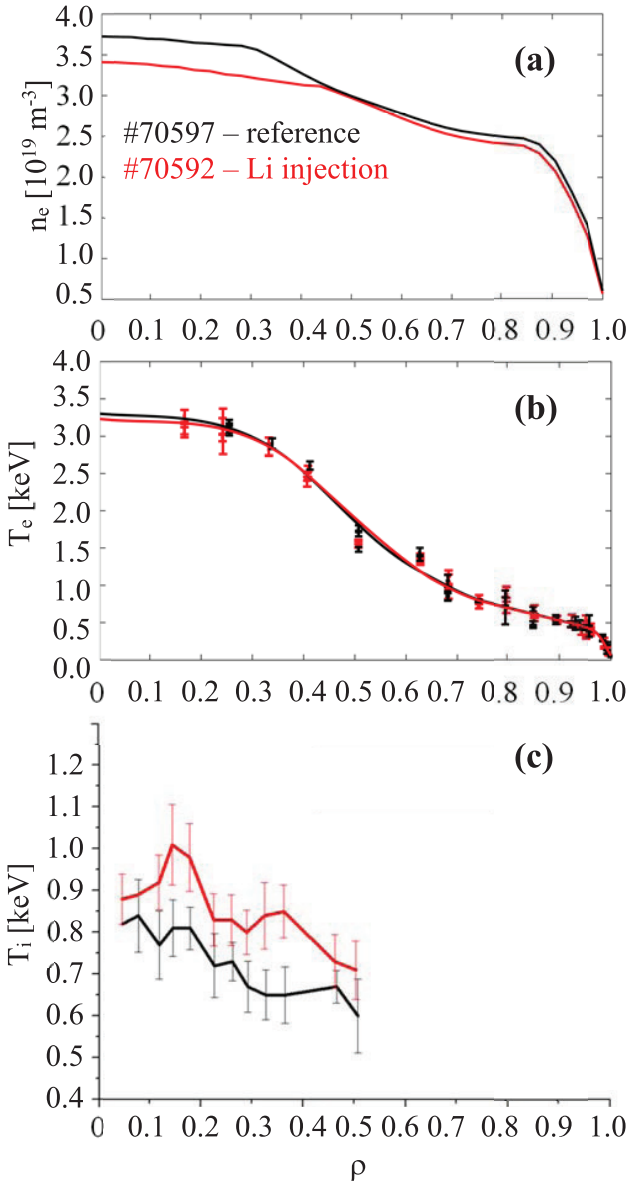

Figure 5. Plasma profile comparison between #70597 and #70592: (*a*) n_e profile from POINT diagnostic at 5.7s, (*b*) T_e profile from Thomson scattering at 5.7s, and (*c*) core T_i from charge exchange recombination spectroscopy at 6.05 s, all as a function of normalized radius, ρ.

edge T_i profile. Thus kinetic equilibria to test the edge stability of these discharges could not be reconstructed, and edge stability assessment is left for future work.

3. Discussion and summary

ELMs have been successfully suppressed in upper-single null H-mode discharges that used the W PFCs as the primary divertor targets, extending previous results that used the lower divertor with graphite PFCs. Moreover these new results show 50% higher energy confinement than the previous results, both in the reference and Li dropper discharges. There is clear evidence of a cumulative wall conditioning effect at constant Li injection rate; ELM elimination improved with the reduced recycling, although a small but modestly increasing price was paid in energy confinement. In effect these experiments can be viewed as a basic existence proof of the ability to eliminate ELMs with high-*Z* PFCs.

For completeness, we mention that in addition to active Li injection, elimination of ELMs is facilitated by at least two other elements in EAST. Density feedback with the supersonic molecular beam injector (SMBI) was disabled in these discharges, as SMBI usage has been previously shown to trigger small ELMs in EAST [43]. Short windows of ELM elimination were observed even with SMBI, but these required higher Li injection rates. In addition vertical oscillations tend to trigger ELMs in EAST, as first reported in Tokamak à Configuration Variable (TCV) [44] and subsequently in other tokamaks. In these discharges vertical oscillations were not present, partly due to the modest I_p and heating power, but vertical oscillations become more common at higher I_p and heating power. Documentation of the role of SMBI and vertical oscillations is being prepared in a longer journal article that will expand on the present results. Control of both of these effects will be crucial in extending the present results.

While the present results show promise, the ELM elimination needs to be extended to higher I_p, higher heating power, and hence lower normalized collisionality ($\nu*$) discharges. Vertical oscillations have hindered the ability for robust ELM elimination in those experiments to date, but substantial effort is going toward further improving the plasma vertical control. Furthermore high quality edge Thomson profiles for data-constrained kinetic equilibria are needed to assess the underlying transport and stability physics. Such high quality profiles and kinetic equilibria are occasionally but increasingly available, and will become a focus of future documentation experiments.

Acknowledgments

This research was supported in part by the U.S. Dept. of Energy Contracts DE-AC02-09CH11466, DE-FG02-09ER55012 and DE-FC02-04ER54698, and partly by the National Key Research and Development Program of China under Contract No. 2017YFA0402500, the National Nature Science Foundation of China under Contract No.11625524, No.11605246, No.11405210 and National Magnetic confinement Fusion Science Program of China under Contract No. 2013GB114004. The digital data for this paper can be found at: http://arks.princeton.edu/ark:/88435/dsp01wp988n475 We gratefully acknowledge the contributions from the EAST technical staff.

ORCID iDs

R. Maingi https://orcid.org/0000-0003-1238-8121
Y.F. Wang https://orcid.org/0000-0002-0368-9566

References

[1] Wagner F. *et al* 1982 *Phys. Rev. Lett.* **49** 1408
[2] Zohm H. *et al* 1994 *Plasma Phys. Control. Fusion* **36** A129
[3] Loarte A. *et al* 2003 *J. Nucl. Mater.* **313–6** 962
[4] Loarte A. *et al* 2007 *Phys. Scr.* **T128** 222
[5] Zohm H. 1996 *Plasma Phys. Control. Fusion* **38** 105
[6] Eich T. *et al* 2017 *Nucl. Mater. Energy* **12** 84
[7] Lang P.T. *et al* 2013 *Nucl. Fusion* **53** 043004
[8] Loarte A. *et al* 2014 *Nucl. Fusion* **54** 033007
[9] Maingi R. 2014 *Nucl. Fusion* **54** 114016
[10] Lang P.T. *et al* 2012 *Nucl. Fusion* **52** 023017
[11] Baylor L.R. *et al* 2013 *Phys. Rev. Lett.* **110** 245001
[12] Mansfield D.K. *et al* 2013 *Nucl. Fusion* **53** 113023
[13] Bortolon A. *et al* 2016 *Nucl. Fusion* **56** 056008
[14] Kallenbach A. *et al* 2010 *Plasma Phys. Control. Fusion* **52** 055002
[15] Beurskens M.N.A. *et al* 2013 *Plasma Phys. Control. Fusion* **55** 124043
[16] Wolfrum E. *et al* 2017 *Nucl. Mater. Energy* **12** 18
[17] Canik J.M. *et al* 2010 *Phys. Rev. Lett.* **104** 045001
[18] Solomon W.M. *et al* 2012 *Nucl. Fusion* **52** 033007
[19] Burrell K.H. *et al* 2001 *Phys. Plasmas* **8** 2153
[20] McDermott R.M. *et al* 2009 *Phys. Plasmas* **16** 056103
[21] Evans T.E. *et al* 2006 *Nat. Phys.* **2** 419
[22] Suttrop W. *et al* 2011 *Phys. Rev. Lett.* **106** 225004
[23] Kugel H.W. *et al* 2008 *Phys. Plasmas* **15** 056118
[24] Bell M.G. *et al* 2009 *Plasma Phys. Control. Fusion* **51** 124054
[25] Mansfield D.K. *et al* 2010 *Fusion Eng. Des.* **85** 890
[26] Hu J.S. *et al* 2015 *Phys. Rev. Lett.* **114** 055001
[27] ITER Physics Expert Group on Confinement and Transport *et al* 1999 *Nucl. Fusion* **39** 2175
[28] Lang P.T. *et al* 2017 *Nucl. Fusion* **57** 016030
[29] Li J. *et al* 2013 *Nat. Phys.* **9** 817
[30] Guo H.Y. *et al* 2014 *Nucl. Fusion* **54** 013002
[31] Federici G. *et al* 2017 *Nucl. Fusion* **57** 092002
[32] Wan B. *et al* 2015 *Nucl. Fusion* **55** 104015
[33] Zuo G.Z. *et al* 2012 *Plasma Phys. Control. Fusion* **54** 015014
[34] Sun Z. *et al* 2014 *Fusion Eng. Des.* **89** 2886
[35] Gong X. *et al* 2017 *Plasma Sci. Technol.* **19** 032001
[36] Maingi R. *et al* 2009 *Phys. Rev. Lett.* **103** 075001
[37] Osborne T.H. *et al* 2015 *Nucl. Fusion* **55** 063018
[38] Canal G.P. *et al* 2017 *IEEE Trans. Plasma Sci.* submitted
[39] Heidbrink W.W., Kim J.C. and Groebner R.J. 1988 *Nucl. Fusion* **28** 1987
[40] Liu H.Q. *et al* 2014 *Rev. Sci. Instrum.* **85** 11D405
[41] Maingi R. *et al* 2012 *Nucl. Fusion* **52** 083001
[42] Canik J.M. *et al* 2017 *IEEE Trans. Plasma Sci.* submitted
[43] Hu J.S. *et al* 2015 *J. Nucl. Mater.* **463** 718
[44] Degeling A.W. *et al* 2003 *Plasma Phys. Control. Fusion* **45** 1637